24PM2D-02

Numerical Green's Function for Radio Frequency Tomography with Complex Geometry

Tadahiro Negishi [#1], Vittorio Picco [#2], Shingo Nishikata [*3], Danilo Erricolo [#4]

[#] *Department of Electrical and Computer Engineering, University of Illinois at Chicago*
Chicago, IL, 60607, USA
[1] tnegis2@uic.edu, [2] vpicco2@uic.edu, [4] derric1@uic.edu

[*] *Mitsubishi Heavy Industry, Ltd.*
Higashi Tanaka, Komaki, Aichi prefecture 485-8561, Japan
[3] shingo.nishikata@gmail.com

***Abstract*—We describe the use of numerical Green's functions applied to Radio Frequency Tomography. RF Tomography relies on a linear operator in matrix form, which depends on a Green's function. The availability of the correct Green's function can be an important limitation when imaging in non-trivial scenarios. If the function cannot be found analytically, numerical methods can be used efficiently. We present simulation results that show the benefit of using a numerical Green's function by comparing it to the result that would be obtained with the analytical function for the homogeneous space.**

I. Introduction

Radio Frequency Tomography is an imaging technology first proposed for underground applications by Wicks [**?**] and later on described in [**?**], [**?**] and [**?**]. This technique is based on multiple, inexpensive, distributed sensors used to reconstruct the contrast dielectric permittivity distribution of the volume under investigation. The goal of RF Tomography is to detect the presence of a target, which could be a tunnel in the case of underground investigations. This technique was conceived to produce images when monochromatic signals are used, therefore an extremely narrow-band electrically small antenna should be employed in Radio Frequency Tomography.

Free space scenarios have been experimentally validated in [**?**], [**?**], [**?**] and [**?**]. Underground scenarios have been tested mostly by means of computer simulations [**?**]. The theoretical model for the underground scenario assumes that the ground is a uniform material, so that the overall geometry can be modeled as a half-space, with a perfectly flat interface between two homogeneous and infinitely extended spaces. This assumption allows to compute the analytic Green's function needed to obtain images.

Despite the good simulation results achieved, it is clear that for an actual implementation of RF Tomography less simplified scenarios must be accounted for. One improvement of RF Tomography to include more realistic scenarios is the investigation of the effects of irregular surfaces, which was investigated in [**?**].

In this paper, we focus on another improvement of RF Tomography where we develop numerical Green's functions to account for more complex scenarios for which Green's function are not available.

II. Method

In RF Tomography, the forward model for the scattered field $\mathbf{E^S}$, based on the Born approximation, is

$$\mathbf{E^S}(\mathbf{t},\mathbf{r}) = Qk_0^2 \int_D [\mathbf{a}_m^r \cdot \underline{\underline{\mathbf{G}}}(\mathbf{r},\mathbf{r}')] \cdot [\underline{\underline{\mathbf{G}}}(\mathbf{r}',\mathbf{t}) \cdot \mathbf{a}_n^t] \epsilon_\delta(\mathbf{r}') d\mathbf{r}', \tag{1}$$

where ϵ_δ is the unknown dielectric permittivity, $\mathbf{a}_m^r$ and $\mathbf{a}_n^t$ are unit vectors representing the direction of polarization of the ideal short dipoles corresponding to the receivers and transmitters, respectively, and $Q = -j\omega\mu_0 \Delta l^t I^t$ for an ideal short dipole. Using the appropriate dyadic Green's functions $\underline{\underline{\mathbf{G}}}(\mathbf{r},\mathbf{r}')$ and $\underline{\underline{\mathbf{G}}}(\mathbf{r}',\mathbf{t})$ is critical to obtain successful image reconstructions. Analytic Green's functions for simple scenarios, such as homogeneous and half-spaces, are available and widely used [**?**]. However, in many cases the Green's function for complicated scenarios cannot be found analytically. Therefore, we show that the Green's function for more general scenarios can be found numerically. Specifically, the numerical Green's function is the total electric field due to ideal dipoles that radiate within an arbitrary background.

$$\mathbf{E^t}\left(\mathbf{r},\mathbf{r^t}\right) = Q\underline{\underline{\mathbf{G}}}\left(\mathbf{r},\mathbf{r^t}\right)\mathbf{a}. \tag{2}$$

The total electric field of equation (**??**) is equivalent to a column of the dyadic Green's function, where $Q\mathbf{a}$ is a fundamental vector. By means of computer simulations, it is possible to compute $\mathbf{E^t}$ for virtually any scenario. Then, the Green's function is readily obtained.

The key step is to be able to efficiently model in the simulator everything that is not considered target. In the underground case, geological knowledge of the area under investigation can provide information regarding the presence of layered formations, large boulders, vein of minerals, or even known underground structures. All the information that can be acquired can become part of the Green's function. Upon collection of scattered field measurement from the antennas, only information related to the target (i.e. unknown, not included in the Green's function) will appear in the final image.

Then, equation (**??**) is expressed in matrix form by discretizing the space of interest

$$\mathbf{E^s} = \mathbf{LV}. \tag{3}$$

Since the matrix $\mathbf{L}$ is usually ill-conditioned, the unknown contrast permittivity vector $\mathbf{V}$ must be found using a regularization technique. In this paper, the Algebraic Reconstruction Technique (which is based on the row action iterative method) is used [**?**].

III. Test conditions and Results

To demonstrate our method, we consider a geometry for which an analytical Green's function is not available, shown in Fig. **??**. This geometry consists of a T-shaped duct, represented using brown color and made of dielectric material with $\epsilon_r = 4$ (similar to the one of dry soil), within which a small metallic target, represented in red, is located. The goal is to develop a numerical Green's function that accounts for the shape of the duct to detect the presence of the target, when the volume containing the duct is surrounded by the transmitter and receiver antennas. We tested the technique by using

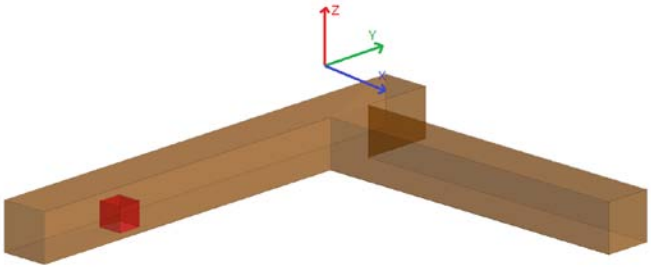

Fig. 1: Problem Geometry: the duct is brown and the PEC target is red.

the commercial simulation software FEKO, which computes both scattered field and numerical Green's function with the Method of Moments. The test conditions involve a single operating frequency of 3.16 GHz, 16 transmitters (modeled as infinitesimal ideal dipoles), and 24 receivers, which are virtually placed by evaluating the scattered field $\mathbf{E^S}$ at those points.

The cubic PEC target has dimensions $1\ \text{cm} \times 1\ \text{cm} \times 1\ \text{cm}$. The duct is composed of two parallelepipedal parts, both having the same cross section 2 cm high and 2 cm wide. Using the reference system indicated in the figure, one vertex of one of the parallelepipeds is located at (-5 cm, -10 cm) and the opposite vertex is located at (-5 cm, 10 cm); the other parallelepiped bisects the first one so that one of its vertices is at (-4 cm, 6 cm) and the other is at (10 cm, 6 cm) in xy-plane. The antennas are all located in the same plane, which is positioned 6 cm above the plane of the duct. The top view of the geometry and location of the antennas is shown in Fig **??**.

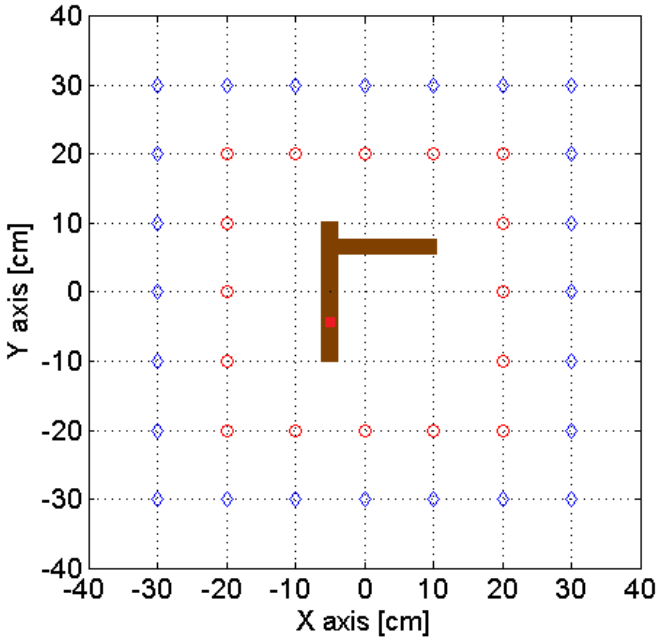

Fig. 2: Problem geometry: the duct and target are at center, the outer blue diamonds are the transmitters, and the inner red circles are the receiver locations.

We tested three cases: PEC target located at (-5 cm, -5 cm),(-5 cm, 6 cm) and (0 cm, 6 cm).

The scattered field is computed with the method of background subtraction. First, the total electric field with duct and the PEC target is computed. Then, the total field without the PEC target is computed. Finally, the scattered field of PEC target is found by subtracting two cases.

Figs. **??**, **??**, **??** show reconstructed images using the free space homogeneous Green's function, which does not account for the presence of the duct. Images based on the numerically computed Green's function are shown in Figs. **??**, **??**, **??**.

When using the homogeneous Green's function, the PEC target appears at an accurate position. The duct does not appear because of background subtraction. Images using numerical Green's function (with the duct) have better contrast and less noise as compared to the previous case. More accurate background information is involved in the imaging process, resulting in a much better resolved image.

IV. Conclusion

In this paper, a method to numerically compute and employ Green's functions is presented. The simulation results demonstrates how to improve models and reconstructed images if obstacles not considered as part of the target are included as background and used to numerically estimate the Green's function.

ACKNOWLEDGMENT

This research was supported by AFRL through grant FA9550-12-1-0174, by RNET and AFRL through grant FA8659010-D-1750, and the UIC Chancellor Undergraduate Research Award.

REFERENCES

[1] M.C. Wicks, "RF Tomography with Application to Ground Penetrating Radars," in *IEEE Proc. 41st Asilomar Conference ACSSC 2007*, Nov. 2007, pp. 2017–2022.

[2] L. Lo Monte, D. Erricolo, F. Soldovieri, and M.C. Wicks, "Radio Frequency Tomography for Tunnel Detection," *IEEE Trans. Remote Sensing and Geoscience*, vol. 48, no. 3, pp. 1128–1137, March 2010.

[3] L. Lo Monte, D. Erricolo, F. Soldovieri, and M.C. Wicks, "RF Tomography for Below-Ground Imaging of Extended Areas and Close-in Sensing," *IEEE Geoscience and Remote Sensing Letters*, vol. 7, no. 3, pp. 496–500, July 2010.

[4] L. Lo Monte, F. Soldovieri, D. Erricolo, and M.C. Wicks, "Imaging Below Irregular Terrain Using RF Tomography," *IEEE Trans. Geosci. Remote Sensing*, vol. 50, No. 9, Sept. 2012, pp. 3364-3373.

[5] V. Picco, T. Negishi, M. Stephens, S. Nishikata, and D. Erricolo, "Experiments for RF Tomography," *National Radio Science Meeting*, Boulder, CO, Jan. 2012.

[6] V. Picco, T. Negishi, S. Nishikata and D. Erricolo, "Comparison of reconstruction algorithms for Microwave Tomography, with applications to experimental data," *IEEE International Symposium on Antennas and Propagation and USNC-URSI National Radio Science Meeting*, Chicago, IL, July 2012.

[7] T. Negishi, S. Nishikata, V. Picco and D. Erricolo, "Advantages of Polarization Diversity in Microwave Tomography," *IEEE International Symposium on Antennas and Propagation and USNC-URSI National Radio Science Meeting*, Chicago, IL, July 2012.

[8] S. Nishikata, V. Picco, T. Negishi and D. Erricolo, "Imaging of dielectric targets using RF Tomography," *IEEE International Symposium on Antennas and Propagation and USNC-URSI National Radio Science Meeting*, Chicago, IL, July 2012.

[9] T. Negishi, V. Picco, and D. Erricolo, "The Use of the Algebraic Reconstruction Technique (ART) for Imaging of Dielectric Targets in Radio Frequency Tomography," *2012 IEEE International Conference on Wireless Information Technology and Systems*, Nov. 2012, Maui, Hawaii, USA.

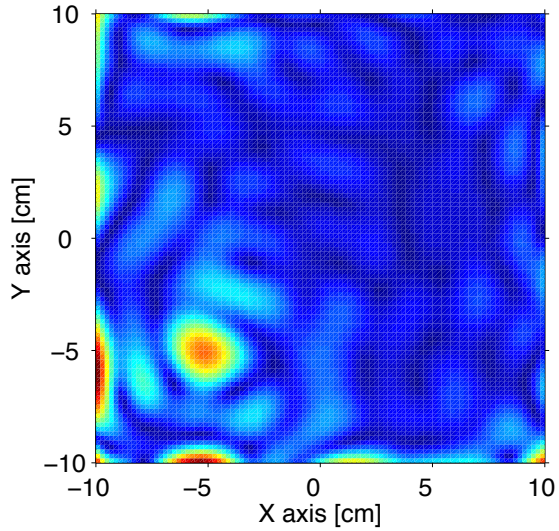

(a) Case 1: homogeneous Green's function with PEC target centered at (-5,5) cm.

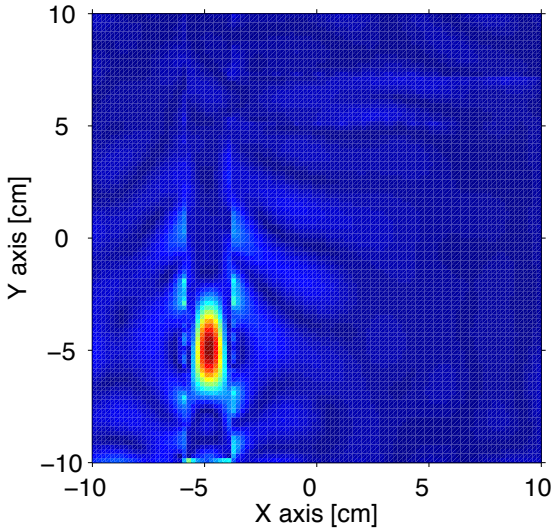

(b) Case 1: numerical Green's function with PEC target centered at (-5,5) cm.

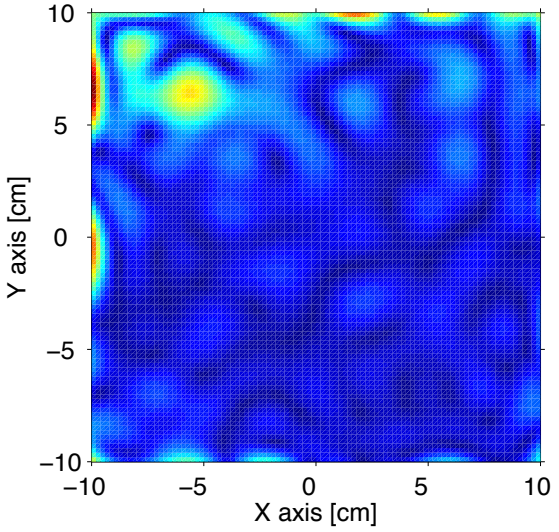

(c) Case 2: homogeneous Green's function with PEC target centered at (-5,6) cm.

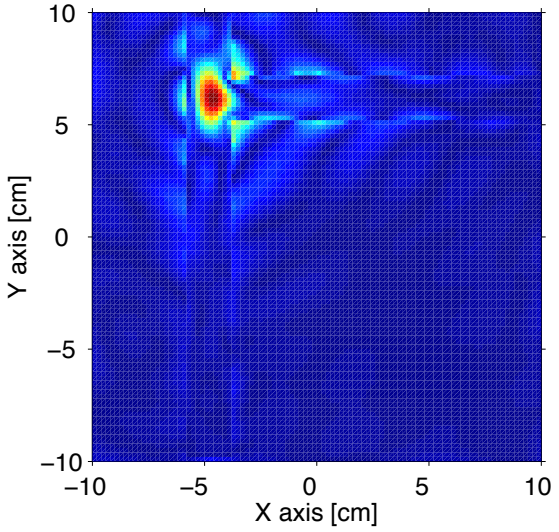

(d) Case 2: numerical Green's function with PEC target centered at (-5,6) cm.

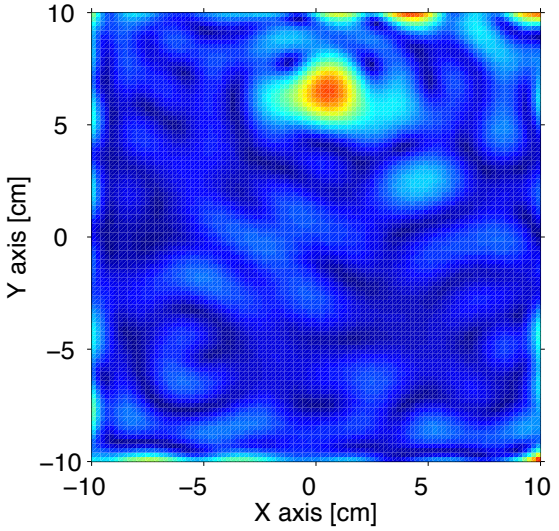

(e) Case 3: homogeneous Green's function with PEC target centered at (0,6) cm.

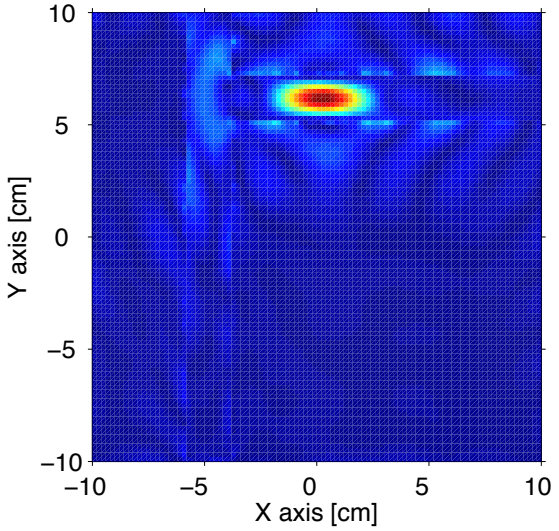

(f) Case 3: numerical Green's function with PEC target centered at (0,6) cm.

Fig. 3: Numerical results.